

Low temperature specific heat in hydrogenated and Mn doped La(Fe,Si)₁₃

Edmund Lovell^{1}, Luis Ghivelder², Amanda Nicotina², Jeremy Turcaud¹, Milan Bratko¹, A. David Caplin¹, Vittorio Basso³, Alexander Barcza⁴, Matthias Katter⁴ and Lesley F. Cohen^{1*}*

¹Blackett Laboratory, Imperial College London, SW7 2BZ, UK

²Instituto de Física, Universidade Federal do Rio de Janeiro, Rio de Janeiro RJ 21941-972, Brazil

³Istituto Nazionale di Ricerca Metrologica, Strada delle Cacce 91, 10135, Torino, Italy

⁴Vacuumschmelze GmbH & Co. KG, Hanau, Germany

It is now well established that the paramagnetic to ferromagnetic transition in the magnetocaloric La(FeSi)₁₃ is a cooperative effect involving spin, charge and lattice degrees of freedom. However, the influence of this correlated behaviour on the ferromagnetic state is as yet little studied. Here we measure the specific heat at low temperatures in a systematic set of LaFe_xMn_ySi_z samples with and without hydrogen, to extract the Sommerfeld coefficient, the Debye temperature and the spin wave stiffness. Substantial and systematic changes in magnitude of the Sommerfeld coefficient are observed with Mn substitution and introduction of hydrogen, showing that over and above the changes to the density of states at the Fermi energy there are significant enhanced d band electronic interactions, at play. The Sommerfeld coefficient is found to be 90-210 mJmol⁻¹K⁻² unusually high compared to that expected from band structure calculations. The Debye temperature determined from the specific heat measurement is insensitive to Mn and Si doping, but increases when hydrogen is introduced into the system. The Sommerfeld coefficient is reduced in magnetic field for all compositions that have a measurable spin wave contribution. These results move our understanding of the cooperative effects forward in this important and interesting class of materials significantly, and provides a basis for future theoretical development.

I. INTRODUCTION

La(Fe,Si)₁₃ based compounds have been widely studied because of their promising magnetocaloric properties associated with a first-order metamagnetic phase transition above the zero field paramagnetic to ferromagnetic Curie temperature (T_C). Substitution of Si for Fe results in increased T_C , lattice contraction and hybridisation between the electronic orbitals of Si and Fe atoms [1,2]. The T_C can also be raised to temperatures close to room temperature by absorption of interstitial hydrogen without significant detriment to the large magnetocaloric effect (MCE) properties [3,4]. This remarkable change is attributed primarily to chemical pressure rather than changes in the band structure, enabling the stabilisation of the ferromagnetic state without significant changes in saturation magnetisation. Partial substitution on the Fe sites by other transition metal elements (Mn, Co, Cr and Ni) and insertion of interstitial atoms such as B, C, N and H have all been explored experimentally. A combination of Mn substitution, which lowers T_C and weakens the first-order character of the phase transition, Si addition and hydrogenation is preferred for optimisation of the magnetocaloric properties, whilst engineering a range of T_C for refrigeration applications [5,6,7,8].

The materials family is also interesting from a fundamental perspective, having giant magnetoelastic coupling, showing as much as 1% change in lattice parameters at the ferromagnetic to paramagnetic transition [1,2]. In recent times there have been new efforts to examine the metamagnetic transition in La(Fe,Si)₁₃ in terms of the itinerant electron metamagnetism (IEM). First principle calculations based on density functional theory (DFT) have been used to study the variation of Si content [9,10] and the effect of interstitial doping [11] and transition metal substitution [12] on the electronic structure and nature of the magnetic interaction. Most recent of these is a study of the thermodynamics of the transition with a particular focus on the pronounced magnetoelastic softening despite the large volume decrease at the transition [13]. These efforts are desirable so that the material properties can be explored

*Authors to whom correspondence should be addressed.

Email: e.lovell12@imperial.ac.uk; l.cohen@imperial.ac.uk

by theoretical combinatorial methods, and also so that a better fundamental understanding is developed of this material system which is one of the important and promising families for use in magnetocaloric cooling technologies.

Here we are motivated to use low temperature specific heat to study the influence of Mn substitution and hydrogenation on the ferromagnetic state of these interesting materials. The low temperature specific heat for a metallic ferromagnet can be well described as:

$$C(T) = \gamma T + \alpha T^{3/2} + \beta T^3 \quad (1)$$

where γ is the prefactor to the linear term normally associated with the electronic specific heat (the Sommerfeld coefficient), α is associated with spin waves for which the spin wave stiffness coefficient D can be derived as:

$$D = k_B^{5/3} (0.113/\delta\alpha)^{2/3} \quad (2)$$

where δ is the density and β is associated with the Debye temperature θ_D where:

$$\theta_D = (12\pi^4 R/5\beta)^{1/3} \quad (3)$$

Significant theoretical progress has been made to describe the electronic properties and the influence of substitution and interstitial occupancy [9-13] in $\text{La}(\text{FeSi})_{13}$, but detailed comparison with experiment is lacking. In order to make better comparison to theory we determine the behaviour of the low temperature specific heat and extract γ , α and θ_D in a series of samples of $\text{LaFe}_x\text{Mn}_y\text{Si}_z$ with and without hydrogen. Changes in magnitude of γ by 140% are observed with Mn substitution and introduction of hydrogen, which we attribute to mass enhancement effects (enhancement of the equivalent mass of d-band electrons). The spin wave contribution after hydrogenation was unmeasurably small.

II. EXPERIMENTAL METHOD

$\text{LaFe}_x\text{Mn}_y\text{Si}_z$ alloys with variable Mn content were prepared by powder metallurgy technique and hydrogenated as described in [6]. The specific compositions are summarised in Table I. Master alloys were prepared by vacuum induction melting followed by mechanical milling steps to produce fine powders. The composition of each alloy was adjusted by blending master alloys with elemental powers. Compaction of the powder blends was performed by cold isostatic pressing. The green bodies were vacuum sintered at around 1100°C followed by an annealing treatment at 1050°C [14]. Hydrogenation was performed on granulate material with a particle size less than 1 mm. The hydrogen absorption was carried out in high-purity H_2 of about 3MPa at 250 C for 5 h [7]. Note that samples M, N and O are the hydrogenated sister compositions to A, B and C respectively. The remaining six compositions are not direct compositional pairs, however F and R have the same Mn content with a small difference in Si/Fe (see Table I).

Specific heat measurements were performed in a Quantum Design PPMS with field range 0 T to 9 T and temperature range 2 K to 400 K using a relaxation method with two different analyses, described as follows. The sample is attached by Apiezon N grease to a platform with a weak thermal link to the temperature bath. At each temperature, a fixed heating power is applied to the platform and sample to raise the temperature to a set temperature T_{set} , then removed allowing the platform and sample to cool in time to the bath temperature via conduction through the weak thermal link. The two resulting curves as a function of time are then fitted using the two-tau method described by Hwang et al. [15], giving the total heat capacity of the sample, platform and grease. A separate measurement is performed without sample to determine the specific heat of the platform and grease, which is then subtracted to give the specific heat of the sample only.

Across a first-order magnetic phase transition, the curve-fitting relaxation method (CFM) breaks down due to substantially varying C_P over the temperature heating and relaxation range, and the latent heat which causes a plateau in $T(t)$ when the sample temperature remains close to constant while the latent heat is released or absorbed [16]. A separate method suggested in Ref [16], known as the slope difference method (SDM), allows continuous extraction of the specific heat across a phase transition from one heating/relaxation curve. For our measurements, close to the phase transition an in-built Quantum Design SDM algorithm was applied to a heating/relaxation curve crossing the phase transition with $T_{set} - T_{initial} = 20$ K. The data are smoothed via a moving average, the value of which requires optimisation and will affect the peak height and width. Here we used a 2 K moving average. Away from the phase transition, the conventional curve-fitting method was used.

To extract the parameters γ , α and β we fit the heat capacity data to Eqn. (1) between 2 K and 14 K. θ_D and D are subsequently obtained from β and α respectively using Eqn. (3) and Eqn. (2) respectively, assuming a density of 7.30 g cm^{-3} for all compositions [17]. Magnetisation measurements were performed using vibrating sample magnetometry in the Quantum Design PPMS with available field 0 T to 9 T between 2 K and 400 K.

III. RESULTS

Table I: Nominal composition of the samples giving the quantity of each element per formula unit, and their T_C . Samples A to F are the non-hydrogenated set and M to R are hydrogenated.

Sample	La	Fe	Mn	Si	H	T_C (K)
A	1	11.22	0.46	1.32	-	116
B	1	11.33	0.37	1.30	-	129
C	1	11.41	0.30	1.29	-	138
D	1	11.49	0.23	1.27	-	150
E	1	11.66	0.12	1.23	-	167
F	1	11.74	0.06	1.20	-	173
M	1	11.22	0.46	1.32	1.65	270
N	1	11.33	0.37	1.30	1.65	285
O	1	11.41	0.30	1.29	1.65	295
P	1	11.54	0.22	1.22	1.65	310
Q	1	11.62	0.15	1.20	1.65	319
R	1	11.76	0.06	1.18	1.65	339

By way of introduction to the magnetic properties of the sample series, Figure 1 shows the temperature dependence of magnetisation for the twelve samples, taken in field cooling and warming in a 1T field. As reported elsewhere [7], the addition of hydrogen raises the magnetic transition temperature; here by 154K, 156K and 157K in samples M, N and O respectively. The magnetic transition is sharpest (most first-order) and has largest hysteresis for the lowest Mn content samples as reported by Basso et al. [18], and this is true for both the hydrogenated and dehydrogenated series [19]. The saturation magnetisation in a 1T field decreases with Mn addition and it was originally suggested that Mn adds antiferromagnetically into the lattice, as simple dilution (substitution of Mn for Fe) is unable to account for the magnitude of the decrease [8]. Recent density functional theory calculations have confirmed this explicitly [12].

The specific heat is shown in Figure 2 for a representative pair of samples of the same composition with and without hydrogen, M and A respectively. Plotted on this wide temperature scale, it can be seen that at temperatures away from their respective T_C , the curves are in close correspondence. It is this

behaviour that led Fujita et al. to comment that the addition of hydrogen does not change θ_D , and to suggest that hydrogenation does not significantly change the electronic or phonon density of states [2]. These comments were made in reference to the fact that the increase of T_C with hydrogenation is primarily a chemical pressure effect. The inset to Figure 2 shows that there are subtle changes in the specific heat as a result of hydrogenation at intermediate and low temperatures, where the electronic term begins to dominate. As we show below, these features result in significant changes to γ and β that change systematically across the series of samples.

Figure 3 shows the low temperature specific heat plotted as C_p/T versus T^2 . The coefficients γ , α and β were extracted from the appropriate fitting for each sample. There is a variation of intercepts (γ) for all samples, and small deviations from linearity are only evident in the non-hydrogenated series below 5 K, showing the emergence of the spin wave $T^{3/2}$ term as it becomes dominant at low T . In order to extract γ , α and β reliably, the data were fitted in the range 2 K to 14 K to avoid deviations from the Debye T^3 approximation at higher temperatures. The results are shown in Figure 4, 5 and 6 and will be outlined briefly then discussed in more detail in the following section. Figure 4(a) shows that there are clear systematic changes in γ with Mn substitution across the sample series. In order to better gauge the influence of Si, results are also shown on two further samples that do not contain Mn, but with different Si content. The γ values for all samples without Mn or with low Mn content are rather similar, with little variation with hydrogen or Si content. Adding Mn increases γ significantly for the dehydrogenated samples, and to a much lesser extent for the hydrogenated counterpart set. The corresponding trend of γ with T_C is shown in Figure 4b, and shows two independent and close-to-linear dependences. Since T_C has a roughly linear dependence on Mn content this is expected. The results in Figure 5 show a consistent increase in θ_D with hydrogenation of approximately 25-30 K (7%), with no clear trend with Mn content within the experimental uncertainties. Any spin wave component α is too small to be extracted reliably for the hydrogenated samples as shown in Figure 6(a). For the non-hydrogenated samples, the spin wave component decreases as Mn is increased, and correspondingly the spin wave stiffness D , following Eqn. (2), increases.

IV. DISCUSSION

There has been considerable interest in understanding the change in electronic properties across the paramagnetic (PM) to ferromagnetic (FM) transition, as the metamagnetic transition is thought to be related to changes in the electronic free energy. The first calculations were made by Kuz'min and Richter [9] on $\text{LaFe}_{12}\text{Si}$, showing that the free energy had several shallow minima and maxima as a function of the magnetisation. Fujita and Yako [10] extended this work to study the influence of Si site occupancy as a function of Si concentration, and Gercsi et al. have developed it further to look at interstitials [11]. Most recently Gruner et al. [13], focused on understanding how the vibrational density of states is influenced by the magnetoelastic coupling across the transition. The value for γ at the magnetic transition emerges from these density functional theory calculations. For example from Gruner et al., the Sommerfeld coefficient for $\text{LaFe}_{11.6}\text{Si}_{1.4}$ is predicted to be $46.3 \text{ mJmol}^{-1}\text{K}^{-2}$ ($56 \text{ mJkg}^{-1}\text{K}^{-2}$) in the PM state and $23.8 \text{ mJmol}^{-1}\text{K}^{-2}$ ($29 \text{ mJkg}^{-1}\text{K}^{-2}$) in the FM state. The large change in the density of states (DOS) across the transition associated with the change of lattice parameters demonstrates the significant contribution of the electronic entropy change to the total entropy change in these itinerant systems. However most striking is the discrepancy with the measured values of γ which we observe experimentally in the ferromagnetic state, which lie in the range $90\text{-}210 \text{ mJmol}^{-1}\text{K}^{-2}$ ($106\text{-}254 \text{ mJkg}^{-1}\text{K}^{-2}$), shown in Figure 4 (here and throughout this report the unit mole is given per formula unit). In principle we should take into account the effects of finite temperature on the energy dependent band structure, but the change in the DOS at T_C and at low temperatures is expected to be relatively subtle compared to the PM to FM transition itself.

Zero temperature density functional calculations [12] predict that the bare electronic density of states increases with Mn substitution, and that for a change of Mn doping from $y = 0$ to $y = 0.5$, γ should change by about 13%. The observations in Figure 4(a) show that without Mn, the data cluster around 80-100 mJmol⁻¹K⁻², which is about a factor of 4 to 5 higher than the DFT calculation [12]. There is clearly a mass enhancement effect (enhancement of the equivalent mass of d-band electrons). Most fundamental studies agree that hydrogen does not strongly affect the density of states at the Fermi level. However, also shown in Figure 4(a) are the results for LaFe_{13-x}Si_x with $x = 1.2$ and 1.6, both non-hydrogenated and with zero Mn content. We see that γ increases with increasing Si content, indicative of an increase in carrier density, although these changes are much less significant than the changes due to Mn addition.

In addition to the mass enhancement for low or zero Mn content samples, there is a second trend evident in Figure 4, a strong systematic increase of γ as Mn is added. For the hydrogenated samples this increase is estimated to be 60% (compared to 13% from DFT) and for the non-hydrogenated set 150% over the same range. In Ref. [5] Wang et al. also discuss the effect of hydrogenation on the magnetic properties, suggesting that it is due mainly to 3d band-narrowing caused by the decrease in the overlap of the Fe 3d orbitals as the distance between the Fe-icosahedral clusters increases. The additional mass enhancement effect, which occurs when Mn is added, is less significant when there is band narrowing in the hydrogenated case.

Interestingly, there are reports in the literature of related itinerant magnetic systems which also have high γ values. Wang et al. studied Nd_xLa_{1-x}Fe_{11.5}Al_{1.5} compounds reporting $\gamma = 193.9$ mJmol⁻¹K⁻² (236 mJkg⁻¹K⁻²) for $x = 0$, and $\gamma = 222.1$ mJmol⁻¹K⁻² (270 mJkg⁻¹K⁻²) for $x = 0.2$ [20]. Enhanced values of γ are thought to be related to strong mass enhancement effects, in these materials brought about by d electron correlations due to spin fluctuations in transition metal ferromagnets [21,22,23], or interband exchange enhancement [24]. It is interesting to note that the mass enhancement is not limited to ferromagnetic compositions only. Michor et al. report $\gamma = 45$ mJmol⁻¹K⁻² (58 mJkg⁻¹K⁻²) theoretically and $\gamma = 200$ mJmol⁻¹K⁻² (256 mJkg⁻¹K⁻²) experimentally in the itinerant strongly exchange enhanced Pauli paramagnet LaCo₉Si₄ [25]. As γ can be written as $\gamma = \pi^2 k_B^2 N(E_F)(1+\lambda)/3$, they estimated a spin fluctuation mass enhancement $\lambda_{\text{spin}} \sim 3.3$. Within similar families of magnetic materials of the NaZn₁₃ structure, an interesting comparison between the itinerant strongly exchange enhanced Pauli paramagnet CeNi₉Si₄ and the compound LaNi₉Si₄ [26], which is a simple Pauli paramagnetic metal, revealed a γ value of 150 mJmol⁻¹K⁻² (192 mJkg⁻¹K⁻²) compared to 33 mJmol⁻¹K⁻² (42 mJkg⁻¹K⁻²), respectively. In this case the mass enhancement is not restricted to ferromagnetic systems, and is likely a result of spin fluctuations. For our materials, we would estimate $\lambda_{\text{spin}} \sim 4.5$ for the low or zero Mn containing samples.

The influence of hydrogen on magnetic properties of La(Fe,Si)₁₃ has been described phenomenologically by Fujita et al [2]. In [2] it is stated that the dominant effect of the hydrogen is not the change in the density of states, but rather the renormalisation due to change in the volume influencing the magnetovolume coupling, and it is this change in magnetovolume coupling that is responsible for the increase in T_C . Using Mossbauer spectroscopy Fujita et al. [27] attributed the change in the magnetic state of LaFe_{13-x}Si_x-H_y solely to the volume expansion caused by hydrogen absorption. Indeed a direct correlation between T_C and unit cell volume due to hydrogenation has already been established [4]. Although the volume expansion leads to a change of the DOS, the role of the additional electrons from the incorporated hydrogen is thought not to affect bands near the Fermi Energy. Previously we have studied the thermopower of LaFe_{11.6}Si_{1.4} and LaFe_{11.6}Si_{1.4}-H_{1.6} across the metamagnetic transition and at low temperatures in order to study the fundamental changes to the electronic density of states at the transition and at low temperatures as a function of hydrogenation [28]. The thermopower data suggest a broadening of the density of states as a result of hydrogenation, and also indicate an additional electron scattering mechanism that enters at low temperatures which could

be suppressed in magnetic field (discussed later). The scattering responsible for the enhanced γ is most likely related to the low temperature features previously observed in the thermopower.

Fujita et al. point out that the changes in T_C with hydrogenation are much more pronounced than the changes in saturation magnetisation [2], and that this trend is precisely what is expected from an itinerant system. They describe the enhancement of the free energy as a function of the magnetisation: at low temperatures the double well potential shows the deepening of the well associated with the FM state and a weakening of the barrier between the FM and PM state. In fact, the recent paper by Gercsi, Fujita and Sandeman looking at the influence of H and other interstitials on the density of states supports this explanation [11]. The band structure calculations show that the free energy well narrows as well as deepens, consistent with an increase of T_C and reduction of spin fluctuations. γ is lower in the hydrogenated compounds, and spin fluctuations are thought to be suppressed in the hydrogenated compounds suggesting that one mechanism producing the enhanced gamma relates to spin fluctuations (and this is consistent with the field dependence of γ discussed below).

Let us now turn to the Debye temperature. The values in Figure 5 show that within the uncertainties of our experiment θ_D increases by about 5 to 10% as hydrogen is incorporated and the lattice expands. Incorporation of hydrogen increases the unit cell volume by about 1% [2]. The absolute value of θ_D depends on the material density and also the average sound velocity, and so on the elastic moduli; thus it is far from straightforward to predict the θ_D from the available experimental data [29]. Nevertheless Fujita et al. [2], determining θ_D from specific heat on $\text{LaFe}_{11.7}\text{Si}_{1.3}$ as a function of hydrogen content, find $\theta_D \sim 350\text{K}$ for all samples. Wang et al., report $\theta_D = 317\text{K}$, 330K and 336K for $\text{LaFe}_{13-x}\text{Si}_x$ with $x = 1.3$, 1.7 and 2 , respectively [30]. Our measurements of θ_D are therefore generally consistent with the literature values adding validity to the fitting process we have used to extract the other parameters discussed in this paper. Between Refs [2] and [30] there is considerable variability for samples of the same nominal composition. The variation in Si site occupancy could affect the absolute value of θ_D . As there are two Fe sites, and in principle the Si site occupancy might depend on sample processing strategy, Fujita and Yako discuss whether there is preferential occupancy, calculating whether one site is more energetically favourable [10]. It is likely that site disorder is a contributing factor to the discrepancies between reported measurements.

The hydrogenated sample set has an unmeasurably small spin wave heat capacity component α (Figure 6(a)); this is also clear from Figure 3 where a deviation from linear fit of C_p/T versus T^2 is absent. In the non-hydrogenated samples there are significant deviations below 5 K due to the finite $T^{3/2}$ term, and the extracted α value shows an increasing trend with Mn doping. The spin wave stiffness D calculated from Eqn. (2) increases with increasing Mn content but the variation across the samples is subtle. Previous measurements of D for $\text{LaFe}_{11.44}\text{Si}_{1.56}\text{H}_x$ calculated from low temperature variations in the magnetisation give $D = 52 \text{ meV } \text{\AA}^2$ for $x = 0$ and $91 \text{ meV } \text{\AA}^2$ for $x = 1.6$ [31]. This result was explained by the increased thermal stabilisation of the FM moment with increased hydrogen content, in tandem to the increase of T_C . Our results are consistent with these findings: the hydrogenated results imply a substantial increase in D which we are unable to reliably calculate from the negligible α component. The samples $\text{LaFe}_{13-x}\text{Si}_x$ with $x = 1.2$ and 1.6 demonstrate that D shows a strong dependence on silicon content.

Finally we move to the field dependence of the specific heat extracted parameters. Figure 7(a) and (b) show the effect of applied magnetic field on γ and θ_D respectively for representative samples C/O, the sister pair with Mn content $y = 0.30$, without and with hydrogen, respectively (extracted using the same fitting as previously, from 2 K to 14 K), and F/R which are the equivalent sister pair with $y = 0.06$. For sample C (F), γ is suppressed with increasing field, whereas in the hydrogenated sample O (R), γ is much less strongly affected. Figure 7(b) suggests that within the error, there is no dependence of θ_D on applied field, as we expect. The field dependences of γ suggested that the enhanced values for γ in the dehydrogenated Mn doped compounds have a magnetic origin, most likely from enhanced scattering

due to spin waves which are suppressed in field. Consistent with this scenario, spin waves were undetected in the hydrogenated samples and in these samples no dependence of γ on field was observed.

V. SUMMARY

We have measured the low temperature specific heat across a series of $\text{LaFe}_x\text{Mn}_y\text{Si}_z\text{H}_v$ compounds and extracted the γ , α and θ_D terms. We find that γ is enhanced in the low Mn doped, hydrogenated samples by a factor of 4 or 5 over band structure DFT calculations, due to effective electronic mass enhancement effects (most probably related to strong electron-lattice coupling). In the Mn containing samples there is a systematic additional dependence of γ on Mn doping which is particularly strong in the dehydrogenated samples. Based on the variation of γ with applied magnetic field, we attribute this contribution to the enhanced γ with Mn doping from an enhanced spin related scattering mechanism. We show an inverse correlation between γ and T_C with two separate gradients for the hydrogenated and non-hydrogenated samples, these provide physical insight into the role of chemical pressure in these compounds. θ_D shows a consistent increase with hydrogenation across the sample set which is independent of composition. Hydrogenation reduces the spin wave component to the heat capacity below our resolution. These results demonstrate that cooperative effects manifest at the paramagnetic to ferromagnetic transition extend down within the ferromagnetic state and suggest that the enhanced interactions we study may provide an interesting playground for other exotic effects when the samples are under hydrostatic pressure for example. The work helps to develop a more complete fundamental understanding of this important and interesting class of materials and provides a basis for future theoretical development.

ACKNOWLEDGEMENTS

This work is in part funded by the European Community's 7th Framework Programme under Grant agreement 310748 "DRREAM", EPSRC EP/G060940/1 and Science Without Borders CAPES grant CSF-PVE's - 88887.063730/2014-00, LG and AN acknowledge addition support from FAPERJ and CNPq.

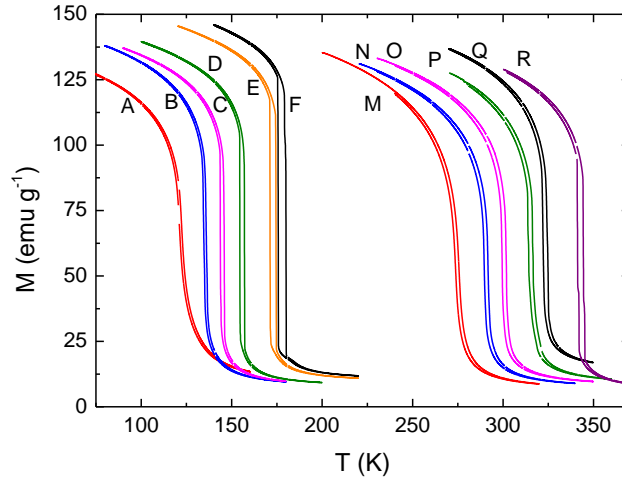


Figure 1: Magnetisation as a function of temperature for the twelve compositions (labelled), six with and six without interstitial hydrogen, in 1 T applied field.

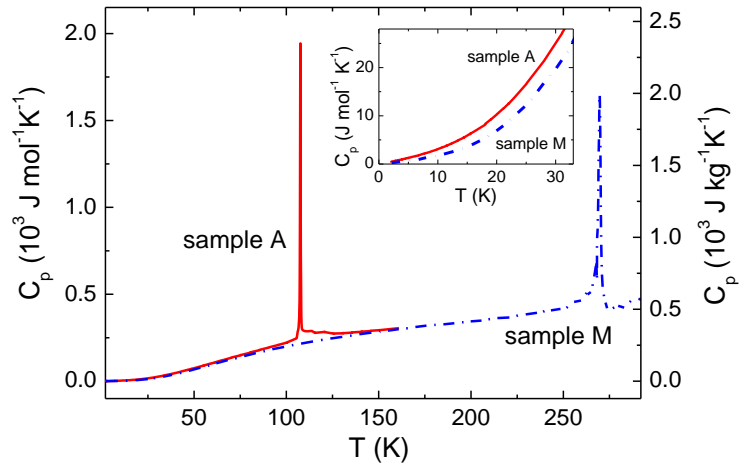


Figure 2: Specific heat $C_p(T)$ for sample A and the hydrogenated equivalent M, in zero magnetic field. Inset shows a blow-up at low temperatures. $C_p(T)$ values were obtained using a combination of curve-fitting relaxation method (CFM) away from the magnetic phase transition at T_C , and slope difference method (SDM) in a small range of temperature (20 K) about T_C , using a moving average of 2 K. See Experimental Section for more details regarding these methods.

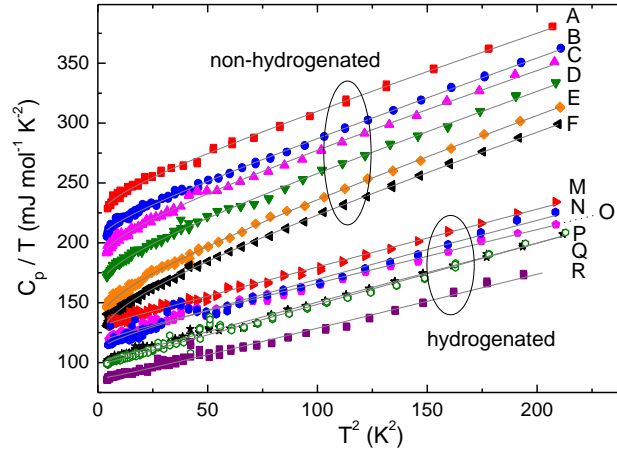


Figure 3: The temperature dependence of C_p/T vs T^2 for all the compositions, showing the data (symbols) and model fittings to Eqn. (1) (lines) between 2 K and 15 K leading to the extraction of γ , α and β .

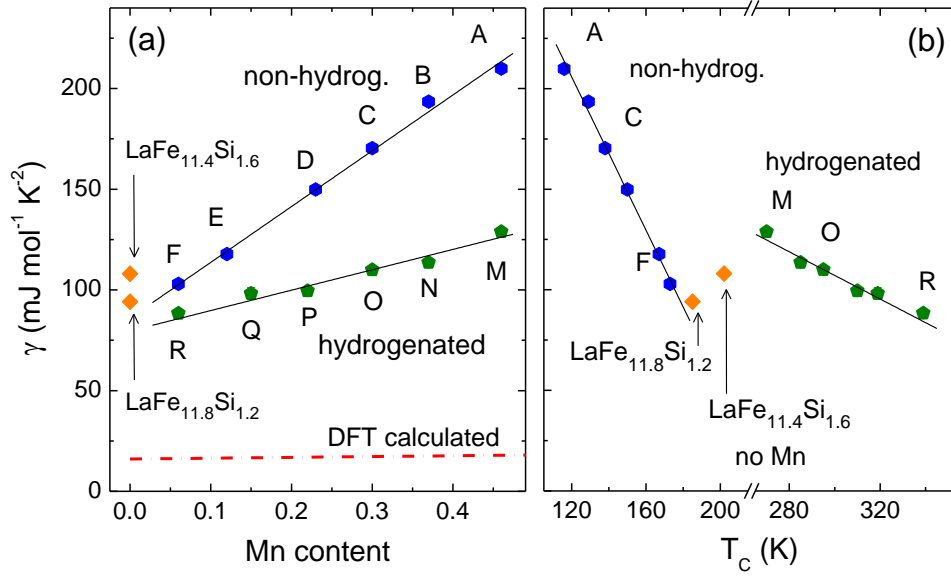


Figure 4: (a) The extracted Sommerfeld coefficient γ as a function of Mn content. The solid lines are a guide to the eye and values of non-hydrogenated and zero Mn content $\text{LaFe}_{11.8}\text{Si}_{1.2}$ and $\text{LaFe}_{11.4}\text{Si}_{1.6}$ are also included. The dashed line is the DFT prediction taken from [12]. (b) The Sommerfeld coefficient as a function of each composition's T_C , also including the compositions $\text{LaFe}_{11.8}\text{Si}_{1.2}$ and $\text{LaFe}_{11.4}\text{Si}_{1.6}$.

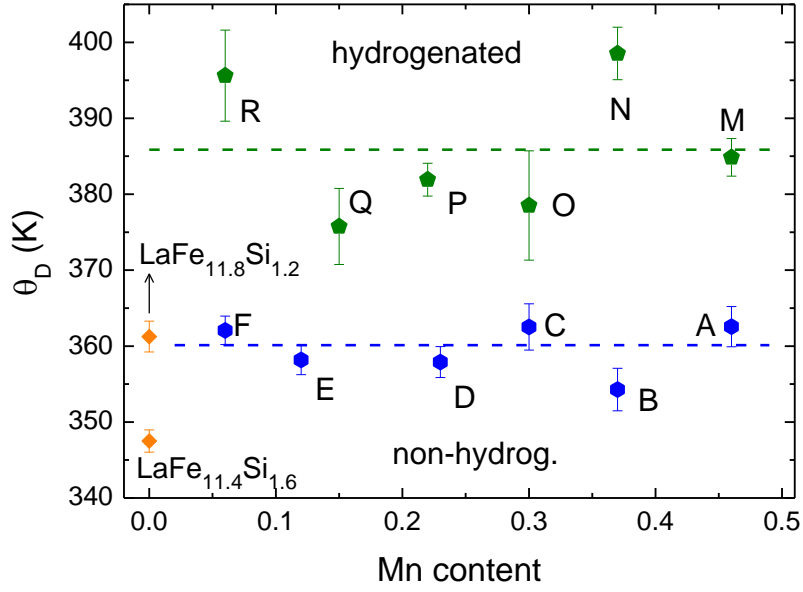


Figure 5: θ_D with Mn composition, as calculated from the coefficient β .

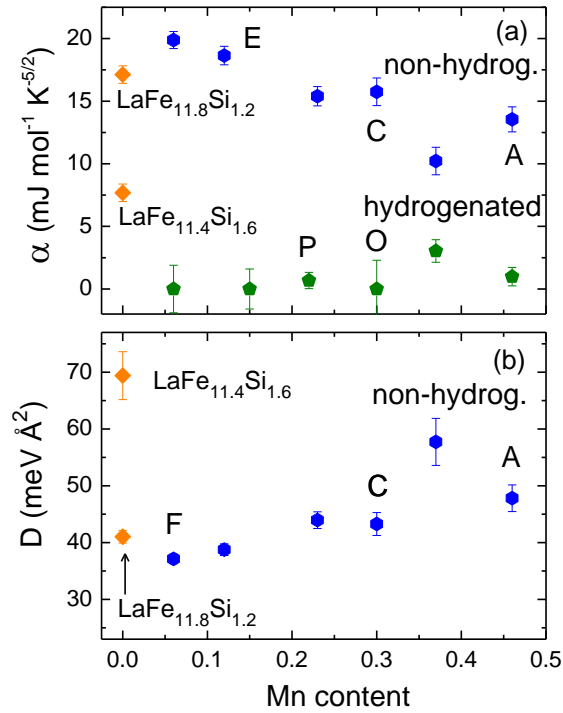


Figure 6: (a) Extracted α for both the hydrogenated and non-hydrogenated composition sets, and (b) Derived spin wave stiffness D values for the non-hydrogenated set only, with Mn content. Also included in both plots are $\text{LaFe}_{11.8}\text{Si}_{1.2}$ and $\text{LaFe}_{11.4}\text{Si}_{1.6}$ obtained in the same way from the low temperature heat capacity measurement (diamonds).

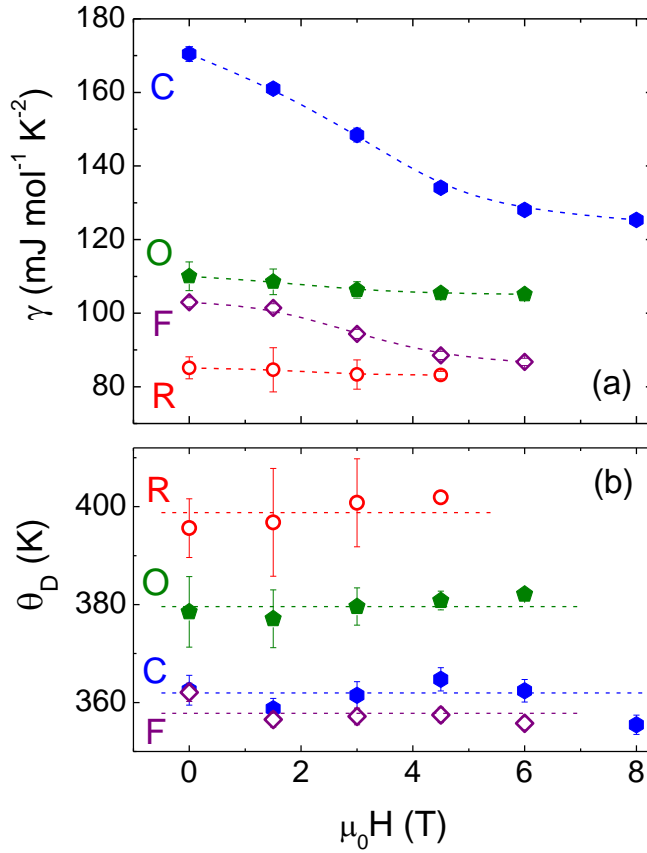


Figure 7: (a) γ and (b) θ_D in field for compositions C, O, F and R, the equivalent composition sets without and with interstitial hydrogen.

¹ A. Fujita and K. Fukamichi, "Giant volume magnetostriction due to the itinerant electron metamagnetic transition in La(Fe-Si)₁₃ compounds." *IEEE Trans. Magn.* **35**, 3796 (1999)

² A. Fujita, S. Fujieda, Y. Hasegawa and K. Fukamichi, "Itinerant-electron metamagnetic transition and large magnetocaloric effects in La(Fe_xSi_{1-x})₁₃ compounds and their hydrides." *Phys. Rev. B* **67**, 104416 (2003)

³ S. Fujieda, A. Fujita, K. Fukamichi, Y. Yamazaki and Y. Iijima, "Giant isotropic magnetostriction of itinerant-electron metamagnetic La(Fe_{0.88}Si_{0.12})₁₃H_y compounds." *Appl. Phys. Lett.* **79**, 653 (2001)

⁴ S. Fujieda, A. Fujita and K. Fukamichi, "Strong pressure effect on the Curie temperature of itinerant-electron metamagnetic La(Fe_{0.88}Si_{0.12})₁₃H_y and La_{0.7}Ce_{0.3}(Fe_{0.88}Si_{0.12})₁₃H_y." *Mater. Trans.* **50**, 483 (2009)

⁵ F. Wang, Y. F. Chen, G. J. Wang, J. R. Sun and B. G. Shen, "Large magnetic entropy change and magnetic properties in La(Fe_{1-x}Mn_x)_{11.7}Si_{1.3}H_y compounds." *Chinese Phys.* **12**, 911 (2003)

-
- ⁶ A. Barcza, M. Katter, V. Zellman, S. Russek, S. Jacobs and C. Zimm, “Stability and magnetocaloric properties of sintered La(Fe,Mn,Si)₁₃H₂ alloys.” *IEEE Trans. Magn.* **47**, 3391 (2011)
- ⁷ M. Krautz, K. Skokov, T. Gottschall, C. S. Teixeira, A. Waske, J. Liu, L. Schultz and O. Gutfleisch, “Systematic investigation of Mn substituted La(Fe,Si)₁₃ alloys and their hydrides for room-temperature magnetocaloric application.” *J. Alloys Compd.* **598**, 27 (2014)
- ⁸ F. Wang, Y. F. Chen, G. J. Wang and B. G. Shen, “The effect of Mn substitution in LaFe_{11.7}Si_{1.3} compound on the magnetic properties and magnetic entropy changes.” *J. Phys. D: Appl. Phys.* **36**, 1 (2003)
- ⁹ M. D. Kuz'min and M. Richter, “Mechanism of the strong magnetic refrigerant performance of LaFe_{13-x}Si_x.” *Phys. Rev. B* **76**, 092401 (2007)
- ¹⁰ A. Fujita and H. Yako, “Stability of metallic, magnetic and electronic states in NaZn₁₃-type La(Fe_xSi_{1-x})₁₃ magnetocaloric compounds.” *Scripta Mater.* **67**, 578 (2012)
- ¹¹ Z. Gercsi, K. G. Sandeman and A. Fujita, “Electronic structure and metamagnetic transition of interstitially doped LaSiFe₁₂.” arXiv:1407.7975[cond-mat.mtrl-sci]
- ¹² Z. Gercsi, “Magnetic coupling in transition-metal-doped LaSiFe_{11.5}TM_{0.5} (TM = Cr, Mn and Ni).” *Europhys. Lett.* **110**, 47006 (2015)
- ¹³ M. E. Gruner, W. Keune, B. Roldan Cuenya, C. Weis, J. Landers, S. I Makarov, D. Klar, M. Y. Hu, E. E. Alp, J. Zhao, M. Krautz, O. Gutfleisch and H. Wende, “Element-resolved thermodynamics of magnetocaloric LaFe_{13-x}Si_x.” *Phys. Rev. Lett.* **114**, 057202 (2015)
- ¹⁴ M. Katter, V. Zellmann, G. W. Reppel and K. Uestuener, “Magnetocaloric properties of La(Fe,Co,Si)₁₃ bulk material prepared by powder metallurgy.” *IEEE Trans. Magn.* **44**, 3044 (2008)
- ¹⁵ J. S. Hwang, K. J. Lin and C. Tien, “Measurement of heat capacity by fitting the whole temperature response of a heat-pulse calorimeter.” *Rev. Sci. Instrum.* **68**, 94 (1997)
- ¹⁶ J. C. Lashley, M. F. Hundley, A. Migliori, J. L. Sarrao, P. G. Pagliuso, T. W. Darling, M. Jaime, J. C. Cooley, W. L. Hults, L. Morales, D. J. Thoma, J. L. Smith, J. Boerio-Goates, B. F. Woodfield, G. R. Stewart, R. A. Fisher and N. E. Phillips, “Critical examination of heat capacity measurements made on a Quantum Design physical property measurement system.” *Cryogenics* **43**, 369-378 (2003)
- ¹⁷ K. A. Gschneidner Jr, V. K. Pecharsky and A. O Tsokol, “Recent developments in magnetocaloric materials.” *Rep. Prog. Phys.* **68**, 1479 (2005)
- ¹⁸ V. Basso, M. K pferling, C. Curcio, C. Bennati, A. Barcza, M. Katter, M. Bratko, E. Lovell, J. Turcaud and L. F. Cohen, “Specific heat and entropy change at the first-order phase transition of La(Fe-Mn-Si)₁₃-H compounds.” *J. Appl. Phys.* **118**, 053907 (2015)
- ¹⁹ M. Bratko, E. Lovell, V. Basso, A. Barcza, M. Katter and L. F. Cohen, “Determining the first-order character of La(Fe,Mn,Si)₁₃.” *preprint*
- ²⁰ F. Wang, J. G. Wang, J. R. Sun and B. G. Shen, “Magnetic properties and magnetocaloric effect in Nd_xLa_{1-x}Fe_{11.5}Al_{1.5}.” *Chinese Phys. B* **17**, 3087 (2008)
- ²¹ M. J. Rice, “Electron-electron scattering in transition metals.” *Phys. Rev. Lett.* **20**, 1439 (1968)
- ²² J. R. Schrieffer, “Effect of virtual spin waves on the properties of strongly paramagnetic metals.” *J. Appl. Phys.* **39**, 642 (1968)
- ²³ A. Fujita, K. Fukamichi, J. T. Wang and Y. Kawazoe, “Large magnetovolume effects and band structure of itinerant-electron metamagnetic La(Fe_xSi_{1-x})₁₃ compounds.” *Phys. Rev. B* **68**, 104431 (2003)
- ²⁴ M. J. Rice, “Itinerant electron correlation and the ideal Lorenz number of transition metals.” *Phys. Lett.* **26A**, 86 (1967)
- ²⁵ H. Michor, M. El-Hagary, M. Della Mea, M. W. Pieper, M. Reissner, G. Hilscher, S. Khmelevskiy, P. Mohn, G. Schneider, G. Giester and P. Rogl, “Itinerant electron metamagnetism in LaCo₉Si₄.” *Phys. Rev. B* **69**, 081404 (2004)
- ²⁶ H. Michor, E. Bauer, M. El-Hagary, C. Dusek, P. Rogl and G. Hilscher, “Kondo-lattice behaviour of CeNi₉Si₄.” *Physica B* **329**, 572 (2003)
- ²⁷ A. Fujita, S. Fujieda and K. Fukamichi, “Influence of hydrogenation on the electronic structure and the itinerant-electron metamagnetic transition in strong magnetocaloric compound La(Fe_{0.88}Si_{0.12})₁₃.” *J. Magn. Magn. Mater.* **321**, 3553 (2009)
- ²⁸ U. Hanneman, J. Lyubina, M. Ryan, N. Alford and L. F. Cohen, *Europhys. Lett.* **100**, 57009 (2012)
- ²⁹ Q. Chen and B. Sundman, “Calculation of Debye temperature for crystalline structures – a case study on Ti, Zr and Hf.” *Acta Mater.* **49**, 947 (2001)

³⁰ G. J. Wang, F. Wang, N. L. Di, B. G. Shen and Z. H. Cheng, "Hyperfine interactions and band structures of $\text{LaFe}_{13-x}\text{Si}_x$ intermetallic compounds with large magnetic entropy changes." *J. Magn. Mater.* **303**, 84 (2006)

³¹ A. Fujita and K. Fukamichi, "Control of large magnetocaloric effects in metamagnetic $\text{La}(\text{Fe}_x\text{Si}_{1-x})_{13}$ compounds by hydrogenation." *J. Alloys Compd.* **404**, 554 (2005)